USAID
FROM THE AMERICAN PEOPLE

USAID SAFE WATER

MANAILE CATCHMENT HYDROLOGIC REPORT

PALAWAN

September 2021

This publication was produced by the USAID Safe Water Project under Contract No. 72049220D00002 and prepared by Geoscience Foundation Inc. as subcontracted by DAI Global, LLC at the request of the United States Agency for International Development. This document is made possible by the support of the American people through the United States Agency for International Development. Its contents are the sole responsibility of the author(s) and do not necessarily reflect the views of USAID or the U.S. Government.

Table of Contents

List of Acronyms

APHRODITE	Asian Precipitation – Highly-Resolved Observational Data Integration Towards Evaluation of the Water Resources
BRS	Bureau of Research and Standards
DOST-PAGASA	Department of Science and Technology – Philippine Atmospheric, Geophysical and Astronomical Services Administration
DPWH	Department of Public Works and Highways
FDC	Flow Duration Curve
GHG	Greenhouse gases
GIS	Geographic Information System
InSAR	Interferometric Synthetic Aperture Radar
JICA	Japan International Cooperation Agency
MGB	Mines and Geosciences Bureau
MO	Manila Observatory
NAMRIA	National Mapping and Resource Information Authority
QGIS	Quantum Geographic Information System
RCP	Representative Concentration Pathway
RS	Remote Sensing
SA-OBS	Observational Gridded Dataset for Southeast Asia

SECTION 1: SURFACE WATER

1.1 Basin Information

The Manaile River, also referred to as Tigman River, is a small river located in the province of Palawan. It is situated in the municipality of Aborlan and has a total drainage area of 39.3 km^2. The climate in the Manaile River Basin is generally categorized as Type 3 under the modified Coronas classification, which has a short dry season between February to April (Figure 1.1). Baseline climate data (i.e., 1976 to 2005) provided by the Manila Observatory indicate a mean annual rainfall of 1,369 mm with a monthly minimum of 27 mm in March and a maximum of 187 mm in October.

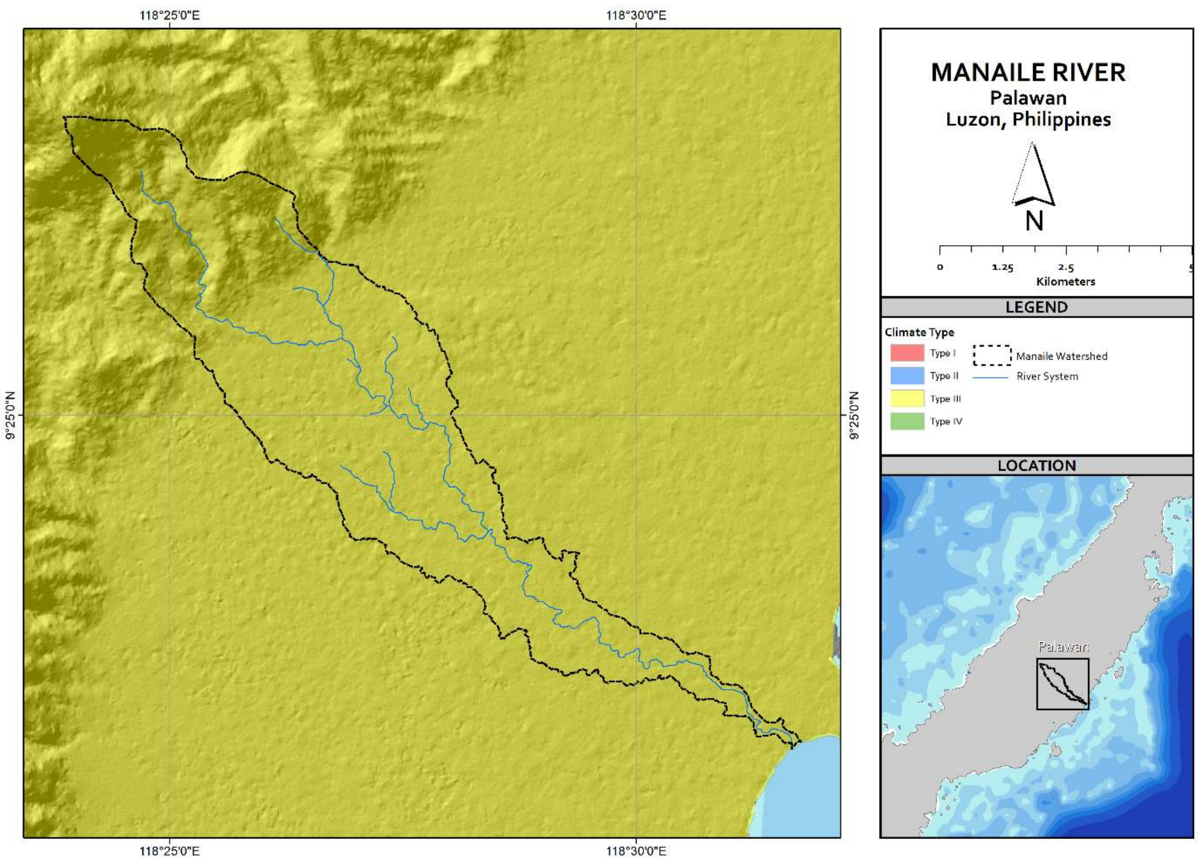

FIGURE 1.1 WATERSHED AND SUB-WATERSHED DELINEATION OF THE MANAILE RIVER BASIN IN A RELIEF MAP. THE WHOLE WATERSHED IS UNDER THE CLIMATE TYPE 3 CLASSIFICATION

1.2 Historical Discharge

The Manaile River is not part of the list of rivers monitored by the DPWH-BRS therefore the reference gauged river used in this study is the larger Batang-Batang River which is southwest of the Manaile River catchment.

The following supplementary information is published with the DPWH-BRS data:

Batang-Batang River
Location: Urduja, Narra, Palawan
Station Code No.: R04B.005
Used Rating Table dated: Monday, August 19, 2019
Doc. Code: DPWH-BOD-WPD-QMSF-22

FIGURE 1.2. GOOGLE MAPS IMAGE OF THE MANAILE RIVER

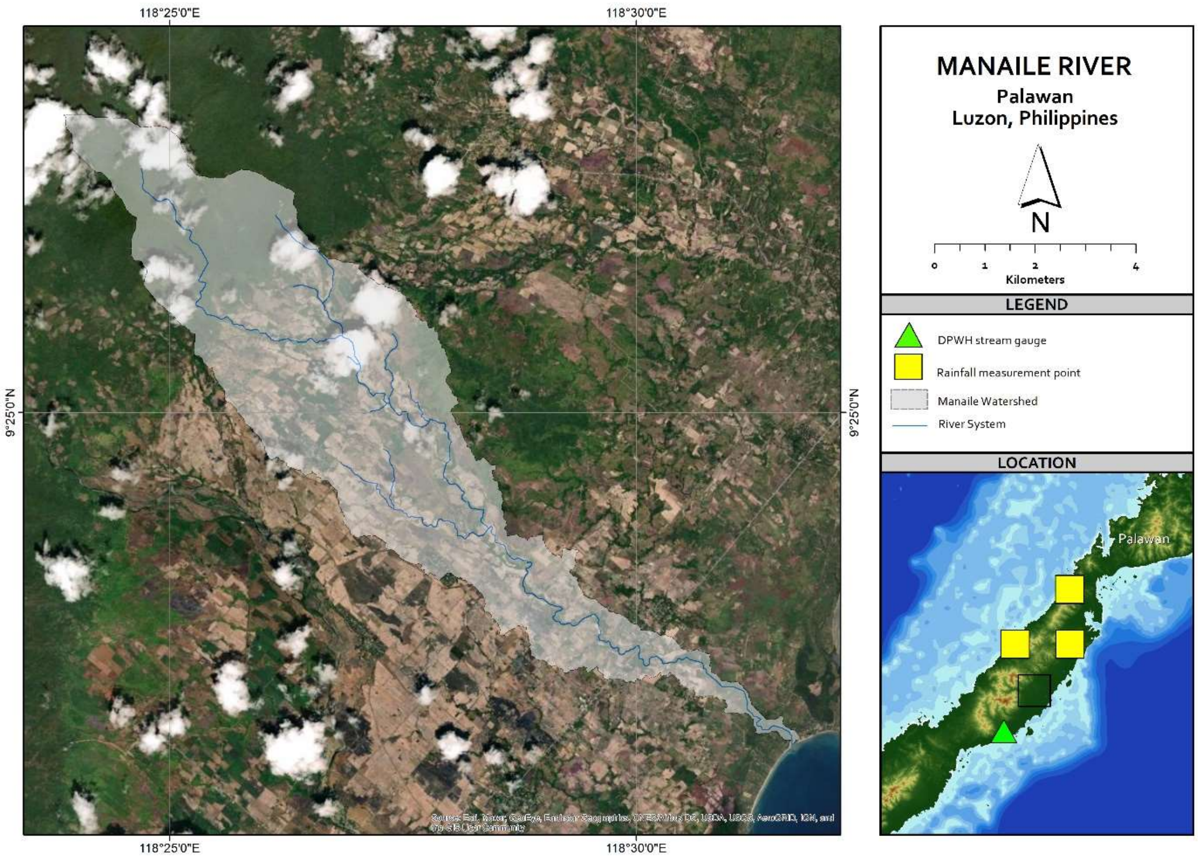

FIGURE 1.3. MAP OF THE MANAILE RIVER BASIN SHOWING THE LOCATION OF THE DPWH STREAM GAUGE AND THE RAINFALL MEASUREMENT POINT (PROVIDED BY THE MANILA OBSERVATORY)

On average, the lowest flows in Batang-Batang River are observed in April with a mean daily discharge of 0.8 $m^3 s^{-1}$ while the maximum flows are observed in December with a mean monthly discharge of 3.3 $m^3 s^{-1}$ (Figure 1.4). The maximum daily flow was recorded in December 2017 at 78.20 $m^3 s^{-1}$ with a corresponding exceedance percentage (i.e., percent of time that this magnitude is equaled or exceeded) of 0.1%. Meanwhile, the lowest daily discharge was recorded in February 2015 at 0.17 $m^3 s^{-1}$, corresponding to a 99.9% exceedance percentage.

The entire flow regime of Batang-Batang River recorded at the DPWH-BRS gauging station is shown in Figure 1.5. The median flow or the discharge that is equaled or exceeded at least 50% of the time (i.e., Q_{50}) is 1.15 $m^3 s^{-1}$, which could be roughly considered as a proxy to the average flow of the river. High flows or discharge values that are equaled or exceeded not more than 20% of the time (i.e., $Q \geq Q_{20}$), start at 2.66 $m^3 s^{-1}$. On the other hand, low flows (i.e., $Q \leq Q_{80}$) start at 0.55 $m^3 s^{-1}$.

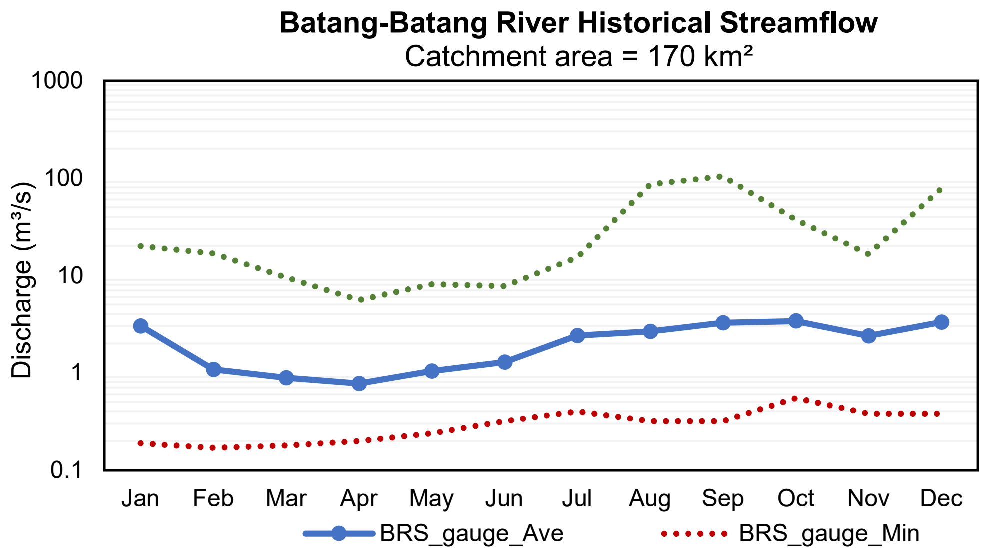

FIGURE 1.4. MONTHLY FLOWS OF BATANG-BATANG RIVER AT THE DPWH-BRS GAUGING STATION

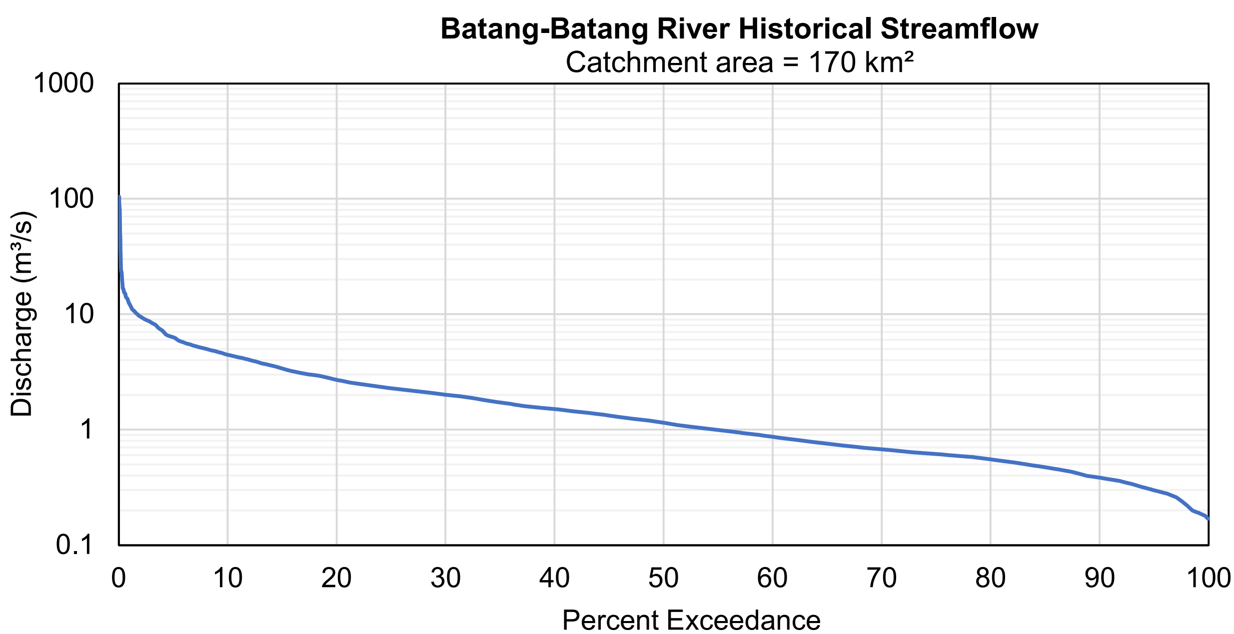

FIGURE 1.5. FLOW DURATION CURVE OF BATANG-BATANG RIVER AT THE DPWH-BRS GAUGING STATION

1.3 Flow Analysis

The flow duration curve is a graphical representation of the flow regime of a stream that shows the percent of time specific discharges were equaled or exceeded during a given period. Flow duration curves (FDCs) are widely used in hydrological and engineering studies related to water resources management. It is a valuable tool for designing irrigation, hydropower, and water supply systems.

In this study, the entire range of stream discharge – from low flows to flood flows – for the whole Manaile River Basin (with a total catchment area of 39.3 km^2) was projected using FDCs. The high flow section of the FDC (i.e., $Q \leq Q_{20}$) is important for hydropower and flood modeling purposes while the low flow section (i.e., $Q \geq Q_{80}$) is used to predict future flows available for water supply.

Three (3) techniques were utilized to create FDCs:

1) Discharge derivation by catchment area transposition;
2) Rainfall – discharge analysis using the rational method; and,
3) Multiple river correlation of rivers in Negros Occidental using regression analyses involving exponential, linear, logarithmic, and power regressions.

Rainfall data provided by the Manila Observatory and stream flow data from DPWH-BRS were used for the flow duration analysis. The details and results of the methods used are described in the succeeding sections.

Method 1: Discharge derivation by catchment area transposition

Method 1 makes use of the catchment area transposition analysis, wherein the flow characteristics of a gauged river are related to the subject river as expressed by the equation:

$$Q = Q_{gauged} * (A/A_{gauged})$$

Where Q is the discharge of the study area ($m^3 s^{-1}$), Q_{gauged} is the recorded discharge of the gauged river ($m^3 s^{-1}$), A is the catchment area of the study area (m^2), and A_{gauged} is the catchment area of the gauged river (m^2). Ideally, the gauged river to be selected as reference should have a robust streamflow record with good data quality and should also bear similar characteristics with the study area including topography, land use, and climate. In this study, the reference river that was used is the Batang-Batang River. The results of Method 1 are summarized in Table 1.1.

TABLE 1.1. RESULTS OF CATCHMENT AREA TRANSPOSITION (REFERENCE: BATANG-BATANG RIVER)

Date	Q_{ref} (m^3 s^{-1})	$Q_{Manaile}$ (m^3 s^{-1})	Flow exceedance
19/12/2017	78.20	18.07	$Q_{0.1}$
23/12/2017	12.08	2.79	Q_1
31/05/2011	6.24	1.44	Q_5
06/08/2010	4.43	1.02	Q_{10}
14/08/2010	2.66	0.61	Q_{20}
30/07/2010	2.02	0.47	Q_{30}
28/08/2010	1.50	0.35	Q_{40}
14/06/2010	1.15	0.27	Q_{50}
28/04/2010	0.86	0.20	Q_{60}
08/04/2010	0.67	0.15	Q_{70}
18/03/2010	0.55	0.13	Q_{80}
30/11/2011	0.38	0.09	Q_{90}
15/01/2012	0.30	0.07	Q_{95}
17/01/2012	0.19	0.04	Q_{99}
18/02/2015	0.17	0.04	$Q_{99.9}$

Method 2: Rainfall – discharge analysis using the rational method

Method 2 utilizes the Rational equation to estimate discharge at the site given its catchment area and precipitation data:

$$Q = ciA$$

Where Q is the discharge of the study area (m^3 s^{-1}), *c* is the runoff coefficient, i is the rainfall intensity (mm $month^{-1}$) and A is the catchment area (m^2). Originally, the equation is designed to calculate peak discharge at a certain rainfall intensity, usually in mm hr^{-1}, wherein the time of concentration is factored in. In this study, the equation is utilized in a straightforward manner - using total monthly precipitation instead to allow direct derivation of mean monthly discharge without the need for a time of concentration.

Monthly rainfall data from 1976 to 2005 was prepared by the Manila Observatory using observed data from DOST-PAGASA and SA-OBS version 2. Average values from the gridded rainfall measurement points were used in this method. Runoff coefficients of 1.0 and 0.2 were selected for January to April and May to December, respectively, from the reference range of 0.55-0.70 for Philippine watersheds with steep gullies and without heavy timber (Table 1.2), considering the general topography of the river basin. The influence of other catchment characteristics (e.g., slope, soil type, land use) and hydrological processes (e.g., infiltration, evapotranspiration) are implicitly accounted for in the runoff coefficient. It is important to note that the adopted approach is highly simplified and is demonstrated primarily for the purpose of comparison with the results of other methods. Nevertheless, this technique is useful in discharge estimation using coarse-resolution datasets/measurements like in the current study. The results of Method 2 are summarized in Table 1.3.

TABLE 1.2. RUNOFF COEFFICIENTS USED IN THE PHILIPPINES PUBLISHED IN THE DESIGN GUIDELINES CRITERIA AND STANDARDS, VOL. 1 (MPWH, 1987)

Surface Characteristics	Runoff coefficient
Lawn, gardens, meadows, and cultivated lands	0.05-0.25
Parks, open spaces including unpaved surfaces and vacant lots	0.20-0.30
Suburban districts with few buildings	0.25-0.35
Residential districts not densely built	0.30-0.55
Residential districts densely built	0.50-0.75
Watershed having steep gullies and not heavily timbered	0.50-0.70
Watershed having moderate slope, cultivated, and heavily timbered	0.45-0.55
Suburban areas	0.34-0.45
Agricultural areas	0.15-0.25

TABLE 1.3. RESULTS OF THE RAINFALL-DISCHARGE ANALYSIS FOR THE MANAILE RIVER BASIN

Year	Month	Mean precipitation (mm)	Q ($m^3 s^{-1}$)	Flow Exceedance
1986	8	265.9	0.81	Q_1
1995	7	219.2	0.66	Q_5
2005	10	197.3	0.60	Q_{10}
1980	12	120.1	0.55	Q_{20}
1994	8	164.6	0.50	Q_{30}
1976	8	152.4	0.46	Q_{40}
2001	12	91.2	0.41	Q_{50}
1980	5	112.5	0.34	Q_{60}
1997	4	48.5	0.22	Q_{70}
1978	4	31.4	0.14	Q_{80}
2001	3	19.1	0.09	Q_{90}
1995	2	15.4	0.07	Q_{95}
1980	3	8.2	0.04	Q_{99}
1976	3	7.1	0.03	$Q_{99.9}$

Method 3: Multiple River correlation of rivers in Palawan using regression analyses

Method 3 adopts multi-river regression analyses wherein the discharge and drainage area of gauged rivers are correlated using different regression techniques such as linear, logarithmic, power, and exponential, and are then used to derive the flow characteristics of the subject river. Ideally, the rivers of reference should (a) be in close proximity to the study area (i.e., within a 50-km radius), (b) have similar climate and catchment characteristics, (c) have clearly defined catchment areas and consistent streamflow records, and (d) have lower and higher catchment areas compared with the study area. However, it is challenging, if not impossible to find reference rivers that fulfill all the qualifications. In this study, three rivers in Palawan were deemed most suitable to use as reference with respect to the abovementioned criteria: Iraan River, Caramay River, and Batang-Batang River (Table 1.4). The coefficient of determination (r^2) was calculated for each analysis. Subsequently, this metric was used to assess the precision of the predicted discharge to the regression trends exhibited by the reference rivers, wherein $r^2 \geq 0.7$ was considered as good correlation. The results of Method 3 are summarized in Table 1.5.

TABLE 1.4. LIST OF PALAWAN ISLAND RIVERS USED AS REFERENCE IN THE REGRESSION ANALYSES

Reference	Coordinates	Location	Catchment area	Streamflow data record
Iraan	10-24-48.94, 119-22-25.21	Brgy. Sto Tomas, Roxas	11.37 km^2	2010-2014, 2017
Caramay	10-10-59.15, 119-13-29.63	Brgy. Caramay, Roxas	94.62 km^2	2010 - 2017
Batang-Batang	9-13-35.92, 118-19-27.65	Brgy. Urduja, Narra	170 km^2	2010 - 2018

TABLE 1.5. RESULTS OF THE REGRESSION ANALYSES FOR THE MANAILE RIVER BASIN. VALUES IN RED DENOTE $R^2 < 0.7$

	Q ($m^3 s^{-1}$)			
Flow exceedance	**Linear**	**Logarithmic**	**Exponential**	**Power**
$Q_{0.1}$	79.84	80.54	79.33	78.12
Q_1	13.10	12.58	12.42	12.04
Q_5	2.64	3.41		7.65
Q_{10}	1.27	1.98	1.24	1.64
Q_{20}	0.74	1.19	0.73	0.99
Q_{30}	0.51	0.87	0.48	0.68
Q_{40}	0.40	0.66	0.37	0.53
Q_{50}	0.33	0.53	0.32	0.43

Q_{60}	0.28	0.42	0.27	0.35
Q_{70}	0.24	0.34	0.22	0.29
Q_{80}	0.18	0.27	0.16	0.22
Q_{90}	0.13	0.20	0.11	0.15
Q_{95}	0.10	0.15	0.08	0.11
Q_{99}	0.06	0.10		
$Q_{99.9}$	0.07	0.02	0.08	0.06

The flow regime projections for the Manaile River Basin using various discharge estimation techniques are shown in Figure 1.6. Among all the methods used, the logarithmic and power regression analyses yielded the highest values in the high flow section of the FDCs while the logarithmic regression technique yielded the highest values in the low flow section. High flows ($Q \geq Q_{20}$) exhibited a wide range of values as expected with a small river with a range of 0.7-1.0 $m^3 s^{-1}$. The median flow is constrained within the range of 0.32-0.43 $m^3 s^{-1}$ and values less than 0.22 $m^3 s^{-1}$ could already be considered as low flow ($Q \leq Q_{80}$) which is also equivalent to NWRB's dependable flow as suggested by historical streamflow data / area transposition analysis.

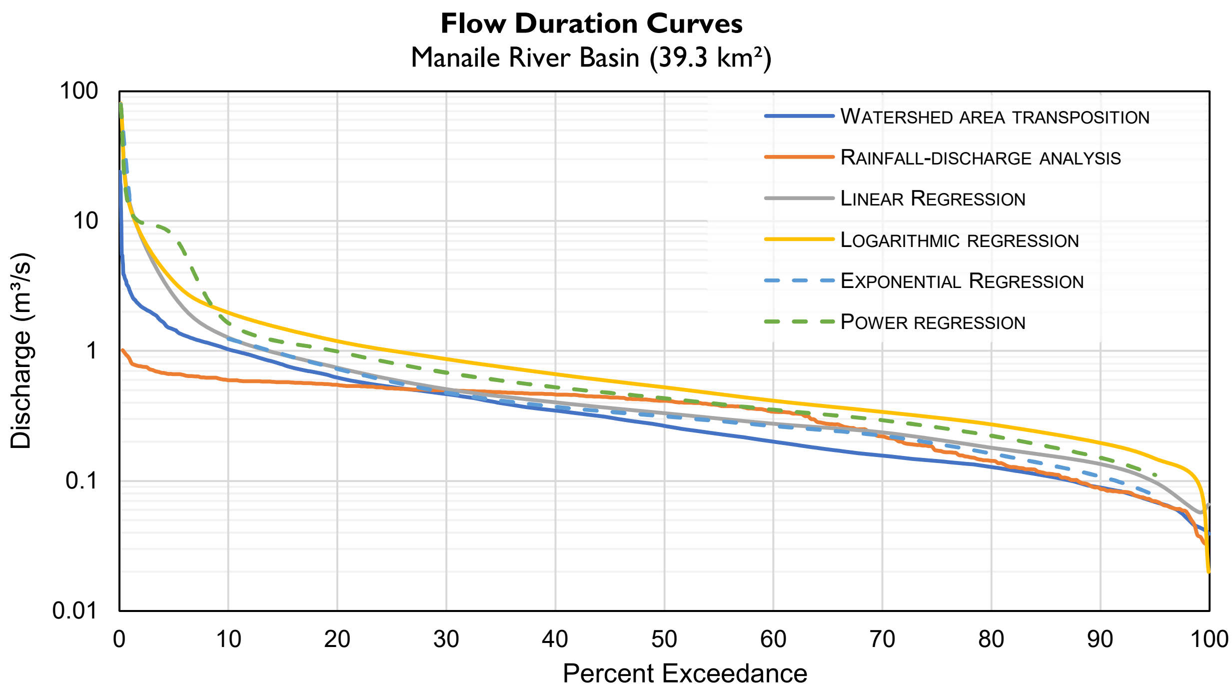

FIGURE 1.6. FLOW DURATION CURVES FOR THE MANAILE RIVER BASIN AS PREDICTED BY VARIOUS ESTIMATION TECHNIQUES

A single permittee for the Manaile River is registered with the NWRB. This is for 0.176 $m^3 s^{-1}$ for the local irrigator's association for irrigation purposes.

TABLE 1.6. REGISTERED WATER RIGHTS PERMITTEE WITH THE NWRB FOR MANAILE RIVER

Province	LGU	Permit	Grantee	Location	Source	Lat	Long	Granted (LPS	Purpose	Grant Date
PALAWAN	ABORLAN	005727	TIGMAN-PLARIDEL I	PLARIDEL, /	TIGMAN RIVER	9.3744	118.4989	176	IRRIGATIC	8/16/1979

1.4 Projection of future flows under different climate scenarios

The Intergovernmental Panel on Climate Change has developed different future scenarios to simulate the impact of greenhouse gas (GHG) emissions on climate. These scenarios are described by the representative concentration pathways (RCP) that are further classified based on the level of end-of-century radiative forcing. Two scenarios were used in this study: (a) RCP 4.5 (representing 4.5 W/m^2 forcing increase relative to pre-industrial conditions) and (b) RCP 8.5 (representing 8.5 W/m^2 forcing increase). In other words, RCP 4.5 is used to predict changes in the climate assuming intermediate GHG emissions, while RCP 8.5 is used to model high GHG effects.

The Manila Observatory has provided bias-adjusted monthly temperature and precipitation values under these two scenarios. Rainfall-discharge analysis was conducted for two future periods, from 2006 to 2035 (i.e., 2020s) and from 2036 to 2065 (i.e., 2050s) Potential hydrological impacts can then be assessed by comparing the baseline flows to the predicted future flows.

The future flow exceedance values and the percentage change for the Manaile River Basin are reflected in Table 1.6. Flows in the RCP 4.5 and RCP 8.5 scenario for the 2020s are mostly expected to decrease except at Q_1-Q_5 (2% to 4% and 3% to 7%, respectively). Both scenarios indicate significant decreases in the lowest flows (-33% to -67%, $Q \leq Q_{99.9}$).

In the 2050s, both the RCP 4.5 and RCP 8.5 scenarios predict considerable flow reduction across the flow regime. Like in the 2020s, both scenarios project significant decrease in the lowest flows in the 2050s.

Note that Table 1.7 only uses the flow exceedance measurements from the rainfall-discharge technique which is directly tied to changes in rainfall volume. Rainfall volume change in turn is what is provided by the various climate change projections. In some cases, the flow exceedances in Table 1.7 (e.g. Q_{80}) will not match with the consensus values discussed in the previous section that included values derived using other techniques particularly the area transposition and the multiple watershed regression analyses. For planning purposes, we report the higher consensus value for high flow conditions (Q_{20}), the full range of median values (Q_{50}), and the lower consensus value for low flow conditions (Q_{80}).

TABLE 1.7. FLOW EXCEEDANCE VALUES (IN $M^3 S^{-1}$) OF FUTURE FLOWS (2006-2035 AND 2036-2065) WITH RESPECT TO THE BASELINE (1976-2005). VALUES IN RED INDICATE NEGATIVE CHANGE FROM THE BASELINE VALUES

Flow exceedance	1976-2005	2006-2035				2036-2065			
	Baseline	RCP 4.5	Change	RCP 8.5	Change	RCP 4.5	Change	RCP 8.5	Change
Q_1	0.81	0.84	4%	0.87	7%	0.74	-9%	0.76	-6%
Q_5	0.66	0.67	2%	0.68	3%	0.62	-6%	0.62	-6%
Q_{10}	0.60	0.59	-2%	0.59	-2%	0.55	-8%	0.57	-5%
Q_{20}	0.55	0.52	-5%	0.51	-7%	0.48	-13%	0.49	-11%
Q_{30}	0.50	0.47	-6%	0.46	-8%	0.44	-12%	0.42	-16%
Q_{40}	0.46	0.44	-4%	0.41	-11%	0.39	-15%	0.38	-17%
Q_{50}	0.41	0.39	-5%	0.37	-10%	0.35	-15%	0.32	-22%
Q_{60}	0.34	0.32	-6%	0.31	-9%	0.27	-21%	0.26	-24%
Q_{70}	0.22	0.14	-36%	0.14	-36%	0.15	-32%	0.13	-41%
Q_{80}	0.14	0.09	-36%	0.09	-36%	0.09	-36%	0.09	-36%
Q_{90}	0.09	0.06	-33%	0.07	-22%	0.06	-33%	0.06	-33%
Q_{95}	0.07	0.05	-29%	0.04	-43%	0.04	-43%	0.04	-43%
Q_{99}	0.04	0.03	-25%	0.02	-50%	0.03	-25%	0.03	-25%
$Q_{99.9}$	0.03	0.02	-33%	0.01	-67%	0.02	-33%	0.01	-67%

The predicted monthly flow statistics (average, minimum, and maximum discharge) in the 2020s and 2050s in both RCP scenarios are illustrated in Figures 1.7 to 1.10. In the RCP 4.5 scenario, reduced average flows are projected for most months during the 2020s, particularly in January (0.15 $m^3 s^{-1}$ to 0.09 $m^3 s^{-1}$) and the dry months of March (0.12 $m^3 s^{-1}$ to 0.08 $m^3 s^{-1}$) and April (0.18 $m^3 s^{-1}$ to 0.11 $m^3 s^{-1}$) where changes of -40%, -33%, and -39% from the baseline of the respective months are calculated. The highest decreases in average flows for the 2050s are also projected in the same months – January (0.15 $m^3 s^{-1}$ to 0.1 $m^3 s^{-1}$), March (0.12 $m^3 s^{-1}$ to 0.07 $m^3 s^{-1}$), and April (0.18 $m^3 s^{-1}$ to 0.1 $m^3 s^{-1}$) are projected, representing 33%, 42%, and 44% reductions from the respective baseline values of each month.

The RCP 8.5 scenario also projects decreased flows for most of the months, with the abovementioned months also projected to have the highest reduction in average flows. For the 2020s, January (0.15 $m^3 s^{-1}$ to 0.1 $m^3 s^{-1}$), March (0.12 $m^3 s^{-1}$ to 0.07 $m^3 s^{-1}$), and April (0.18 $m^3 s^{-1}$ to 0.1 $m^3 s^{-1}$) represent 33%, 42%, and 44% reductions from the respective baseline values of each month. Meanwhile, in the 2050s, January (0.15 $m^3 s^{-1}$ to 0.1 $m^3 s^{-1}$), March (0.12 $m^3 s^{-1}$ to 0.08 $m^3 s^{-1}$), and April (0.18 $m^3 s^{-1}$ to 0.09 $m^3 s^{-1}$) represent 33%, 33%, and 50% reductions from the respective baseline values of each month. The monthly discharge values (average, minimum, maximum) for the baseline and RCP climate change scenarios are shown in Table 1.8.

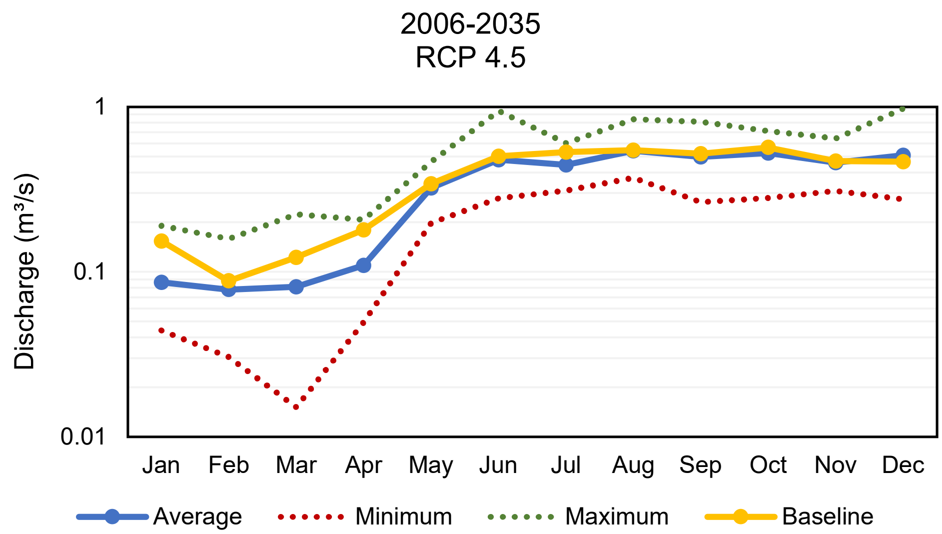

FIGURE 1.7. PREDICTED MONTHLY FLOWS FROM 2006 TO 2035 FOR THE MANAILE RIVER BASIN USING THE RCP 4.5 SCENARIO

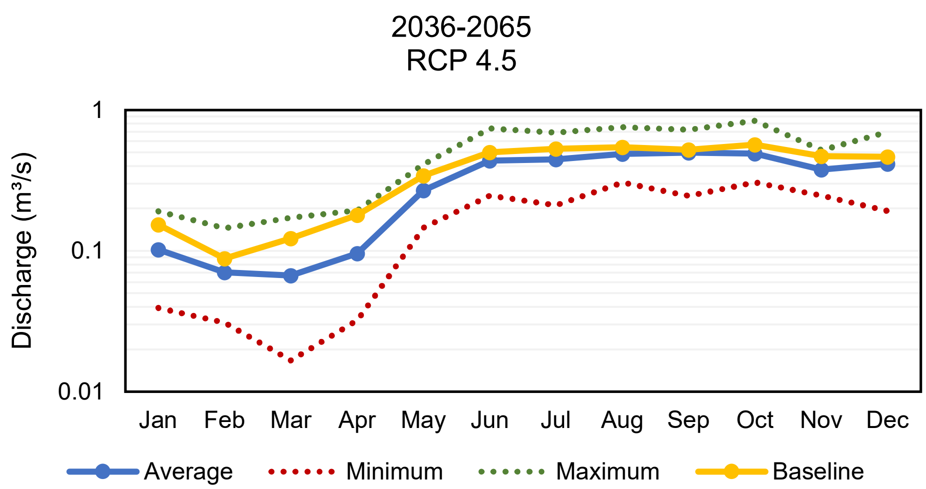

FIGURE 1.8. PREDICTED MONTHLY FLOWS FROM 2036 TO 2065 FOR THE MANAILE RIVER BASIN USING THE RCP 4.5 SCENARIO

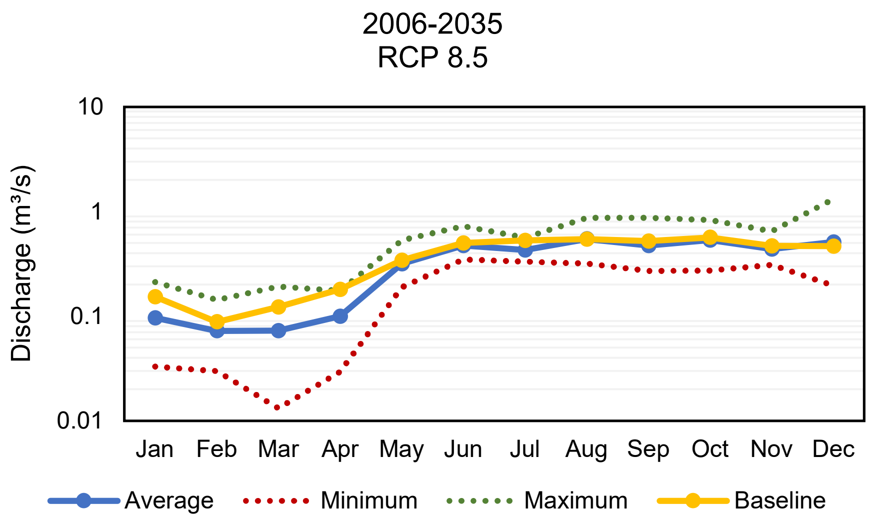

FIGURE 1.9. PREDICTED MONTHLY FLOWS FROM 2006 TO 2035 FOR THE MANAILE RIVER BASIN USING THE RCP 8.5 SCENARIO

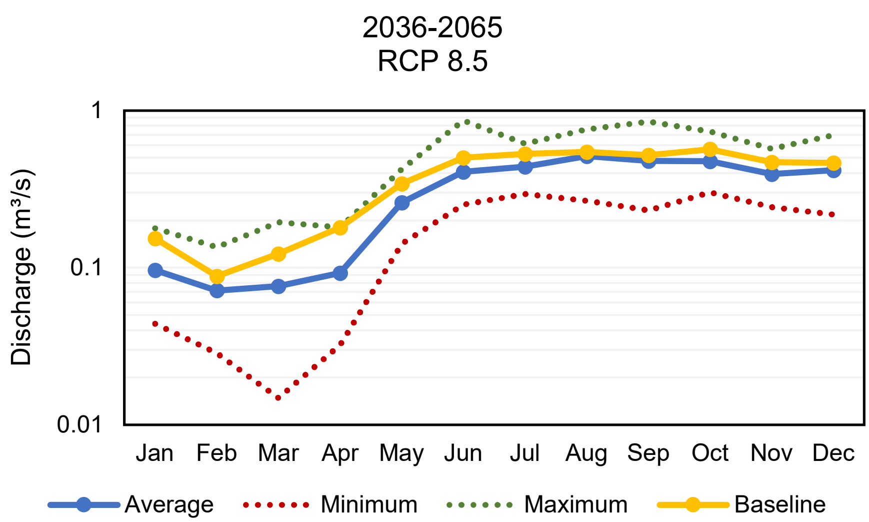

FIGURE 1.10. PREDICTED MONTHLY FLOWS FROM 2036 TO 2065 FOR THE MANAILE RIVER BASIN USING THE RCP 8.5 SCENARIO

TABLE 1.8. MONTHLY DISCHARGE VALUES FOR BASELINE, RCP 4.5, AND RCP 8.5 CLIMATE CHANGE SCENARIOS

Month	Baseline			RCP 4.5						RCP 4.5					
	1976-2005			2006-2035			2036-2065			2006-2035			2036-2065		
	Ave	Min	Max	Ave	Min	Max	Ave	Min	Max	Ave	Min	Max	Ave	Min	Max
Jan	0.15	0.06	0.35	0.09	0.04	0.19	0.10	0.04	0.19	0.10	0.03	0.21	0.10	0.04	0.18
Feb	0.09	0.05	0.17	0.08	0.03	0.16	0.07	0.03	0.15	0.07	0.03	0.14	0.07	0.03	0.14
Mar	0.12	0.03	0.33	0.08	0.02	0.22	0.07	0.02	0.17	0.07	0.01	0.19	0.08	0.01	0.19
Apr	0.18	0.08	0.37	0.11	0.05	0.21	0.10	0.03	0.19	0.10	0.03	0.18	0.09	0.03	0.18
May	0.34	0.21	0.46	0.32	0.20	0.46	0.27	0.15	0.41	0.32	0.19	0.53	0.26	0.14	0.43
Jun	0.50	0.34	0.75	0.48	0.28	0.95	0.44	0.25	0.74	0.47	0.35	0.73	0.41	0.25	0.87
Jul	0.53	0.42	0.70	0.44	0.31	0.60	0.45	0.21	0.69	0.43	0.33	0.56	0.44	0.29	0.61
Aug	0.54	0.42	0.81	0.54	0.37	0.84	0.49	0.31	0.76	0.55	0.32	0.87	0.51	0.27	0.76
Sep	0.52	0.27	0.76	0.50	0.26	0.81	0.50	0.25	0.73	0.47	0.27	0.87	0.48	0.23	0.85
Oct	0.57	0.38	0.77	0.52	0.28	0.71	0.49	0.31	0.84	0.53	0.27	0.83	0.48	0.30	0.74
Nov	0.47	0.26	0.73	0.46	0.31	0.64	0.38	0.25	0.52	0.44	0.31	0.65	0.39	0.24	0.57
Dec	0.47	0.29	1.02	0.51	0.28	0.98	0.41	0.19	0.70	0.51	0.20	1.32	0.42	0.22	0.70

SECTION 2: GROUNDWATER

2.1 Potential Groundwater Recharge Areas

Groundwater recharge, or the process that describes the flow of water from surface sources (e.g., direct from precipitation, streamflow) to the aquifers deep beneath the ground, is still a significant source of freshwater (30%) around the world. In the Philippines, the average proportion of precipitation that ultimately infiltrates as groundwater is between 15-25%, primarily varying based on the prevailing geology and land cover of a particular area. In alluvial areas in humid tropics, the proportion of rainfall ultimately infiltrating shallow aquifers may be as high as 40-45% (Kotchoni et al., 2018).

Although a substantial amount of freshwater is stored as groundwater, finding and developing this resource require significant investments in the exploration of potential groundwater sources. Numerous techniques have been developed over the years to directly and indirectly measure the amount of groundwater entering aquifers. As Yeh et al. (2009) pointed out, on-site hydrogeological investigations and geophysical surveys generally downplay large-scale processes contributing to the dynamics of groundwater recharge. Most of the time, these and other similar techniques rely on just a single (or a few) parameter to estimate recharge.

We identified the geology of the area, topographic slope, drainage density, and land cover as the controlling variables influencing groundwater recharge as used and verified by Shaban et al. (2006), Yeh et al. (2009), Kourgialas and Karatzas (2015), Deepa et al. (2016), and Senanayake et al. (2016). Accordingly, we adopted their approach in using Geographic Information System (GIS) and Remote Sensing (RS) to integrate these variables.

These areas were delineated on the basis of four factors: drainage density, slope gradient, surface lithology, and land cover. The weight of these factors are based on the influence they have on one another. Figures 2.1 and 2.2 illustrate the flowchart representing the methodology of this investigation and the inter-influence of the factors used in determining their corresponding weights. Each primary variable was assigned a numerical weight, signifying its relative importance in promoting infiltration and percolation of water towards the ground. Geology was assigned 34%, land cover with 25%, slope with 25%, and drainage density with 16%; with these weight distribution modified and adapted from Shaban et al., (2006) and Yeh et al., (2009). Subclasses of each primary variable were also allocated with weights according to their likely influence on groundwater recharge.

Zones were classified whether they have very low, low, moderate, high, or very high potential for groundwater recharge. For example, around 40-50% of the total amount of recharge are capable of infiltrating towards the aquifers in very high recharge areas. Conversely, in poor recharge areas less than 5% of estimated recharge is expected to ultimately feed the aquifers. Potential recharge of the areas were classified into five zones: very low recharge for areas with values of 0-20; low recharge areas (20-40) moderate recharge for areas with values of 40-60; good recharge for areas with values of 60-80; and values between 80-100 for very high recharge zones.

The points of these factors were identified by classifying and ranking them on the basis of their influence on the groundwater potential. Using spatial analysis, the factors were then added together and the potential groundwater recharge zones were demarcated. For the determination of the weights of factors, major and minor inter-influences were compared. A major effect or influence equates to one point, while a minor effect or influence equates to a half point. From these the drainage density factor has a weight of 1, lithology has a weight of 2, and both land cover and slope gradient have weights of 1.5. Normalizing these to a hundred points, these weights may be obtained: 16 for drainage density, 34 for lithology, 25 for land cover, and 25 for slope gradient.

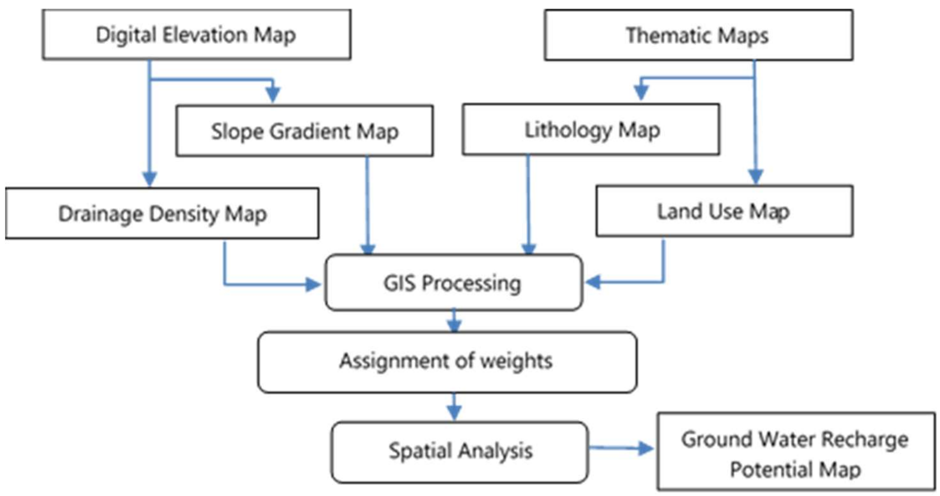

FIGURE 2.1. FLOWCHART FOR DETERMINING POTENTIAL GROUNDWATER RECHARGE ZONES

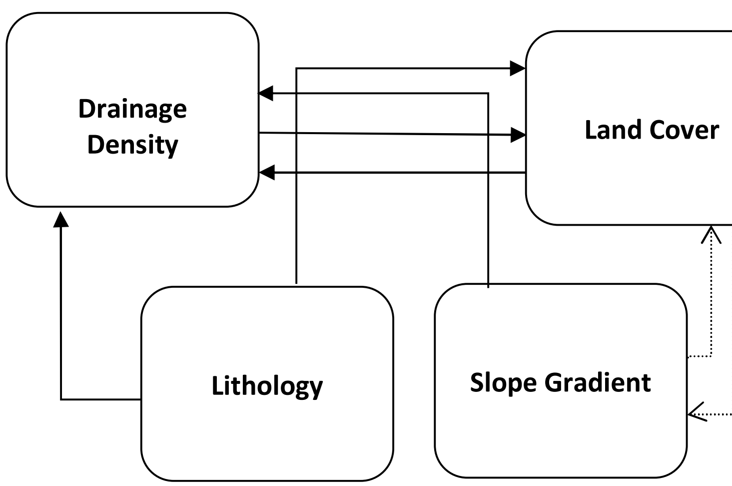

FIGURE 2.2. RELATIONSHIP AMONG VARIABLES (SOLID LINES INDICATE MAJOR EFFECTS, WHILE DASHED LINES REPRESENT MINOR EFFECTS)

A. Drainage Density

Drainage Density is defined as the number of channels in a given sub-catchment per unit area. It is a measure of how well or poorly drained a given sub-catchment is. This has bearing on planning purposes such as delineating areas where groundwater infiltration occurs. The same areas may also be flood-prone areas during the rainy season. Its value may be calculated as the quotient of total length of a channel in a basin and the area of the catchment basin. For this report, drainage density was computed as the ratio between the total length (m) of streams and the total area (sq. km.) of a sub-catchment.

The drainage network and catchment basins of the Manaile River Basin were provided by USAID Safe Water. The drainage density values were calculated and assigned to each respective catchment basin (Figure 2.3).

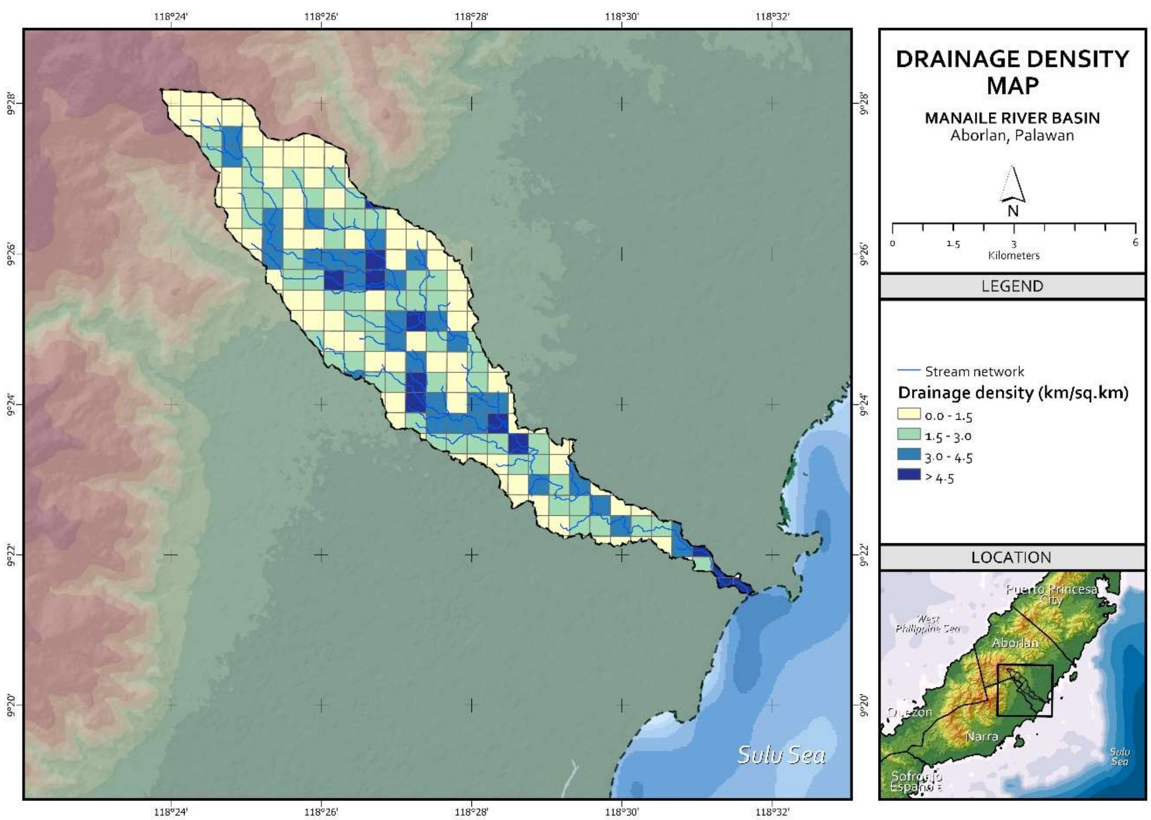

FIGURE 2.3. DRAINAGE DENSITY MAP OF THE MANAILE RIVER BASIN

B. Slope Gradient

The slope gradient influences groundwater recharge by dictating the behavior of rainfall as it flows above ground. As local rainfall is the main source of recharge, slope gradient determines the amount of water that effectively infiltrates the ground. Steep slopes result to little recharge because it causes rainwater to become runoff. On the other hand, gentler slope gradients provide enough time for water to eventually infiltrate the surface and reach the water table.

Slope gradient (in degrees; Figure 2.4) was processed from the 5-meter resolution Interferometric Synthetic Aperture Radar (InSAR) digital elevation model using the slope function of QGIS. Hydrologic and topographic corrections, such as filling in sinks, were done before processing the data into its derivative products.

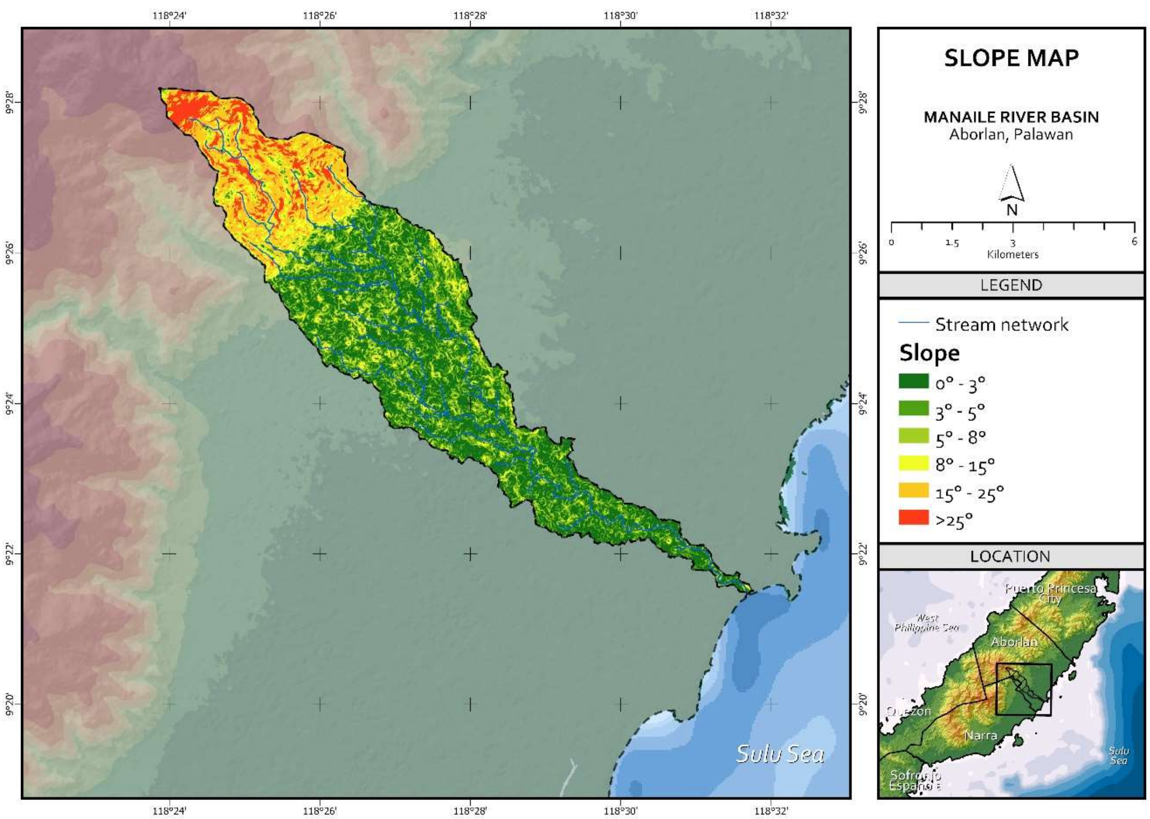

FIGURE 2.4. SLOPE MAP OF THE MANAILE RIVER BASIN

C. Land Cover

The land cover of a particular area partly determines the amount of infiltration of surface water to the water table. The land cover describes the extent of concreted residential areas, the type and extent of vegetation cover, the type of soil deposits, and the presence or absence of any water bodies. Concreted or built-up areas are zones with the least amount of infiltration due to the inability of surface water to penetrate concrete. On the other hand, areas with rich vegetation allow high amounts of infiltration due to the fact that the roots of these plants loosen the overlying rocks and soil- making it easier for water to percolate towards the water table. The type of vegetation present is also an important factor since vegetation with deep roots provide stronger infiltration as compared to vegetation with shallow roots. The amount of foliage in trees also affect recharge potential. Areas with thick foliage may provide a buffer for rainfall due to the droplets being intercepted by plant leaves. Thus, the underlying soil is provided with more time to soak up the rainfall. Furthermore, vegetation with a large area coverage prevents the direct evapotranspiration of water from the soil.

The 2020 land cover of the Manaile River Basin (Figure 2.5) used here were provided by USAID Safe Water, using Landsat 8 images after radiometric calibration and correction.

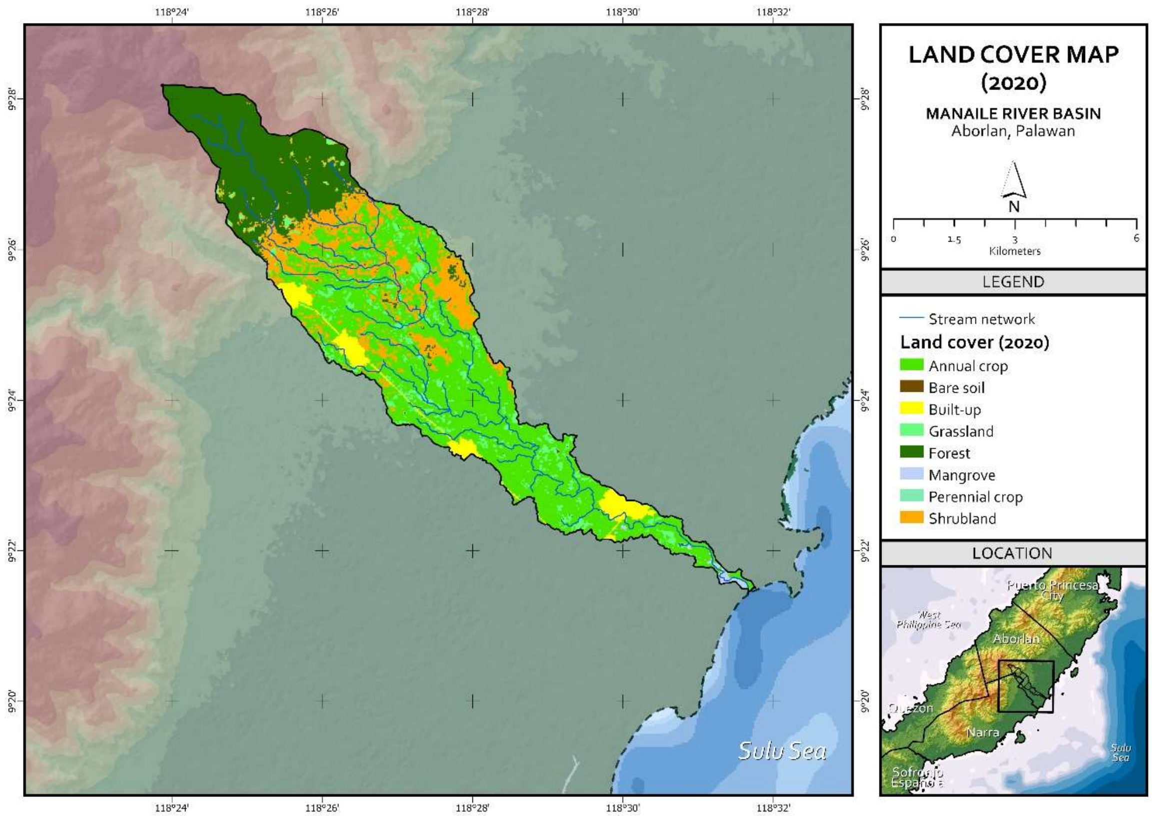

FIGURE 2.5. LAND COVER MAP (2020) OF THE MANAILE RIVER BASIN

D. Lithology

The lithology of the underlying rocks also influences the rate of infiltration to groundwater. Factors affecting the ranking of different lithologies are its porosity and permeability. In general, for sedimentary rocks, a larger grain size means a higher permeability. Meanwhile, for igneous and metamorphic rocks, the permeability is determined by the susceptibility of the rock to break or fracture- creating spaces within the rock for groundwater to fill up.

The lithology of the river basin (Figure 2.6) was delineated and digitized from existing geologic maps of National Mapping and Resource Information Authority (NAMRIA), the Mines and Geosciences Bureau (MGB), and based on the more recent geologic maps of Neri et al. (2013). Weights for each lithologic unit were assigned based on the geologic age and texture of each unit. Thus, Quaternary alluvium and sandstones formed during Miocene were expected to facilitate infiltration and recharge of precipitation than claystones and igneous intrusions from Cretaceous, for example.

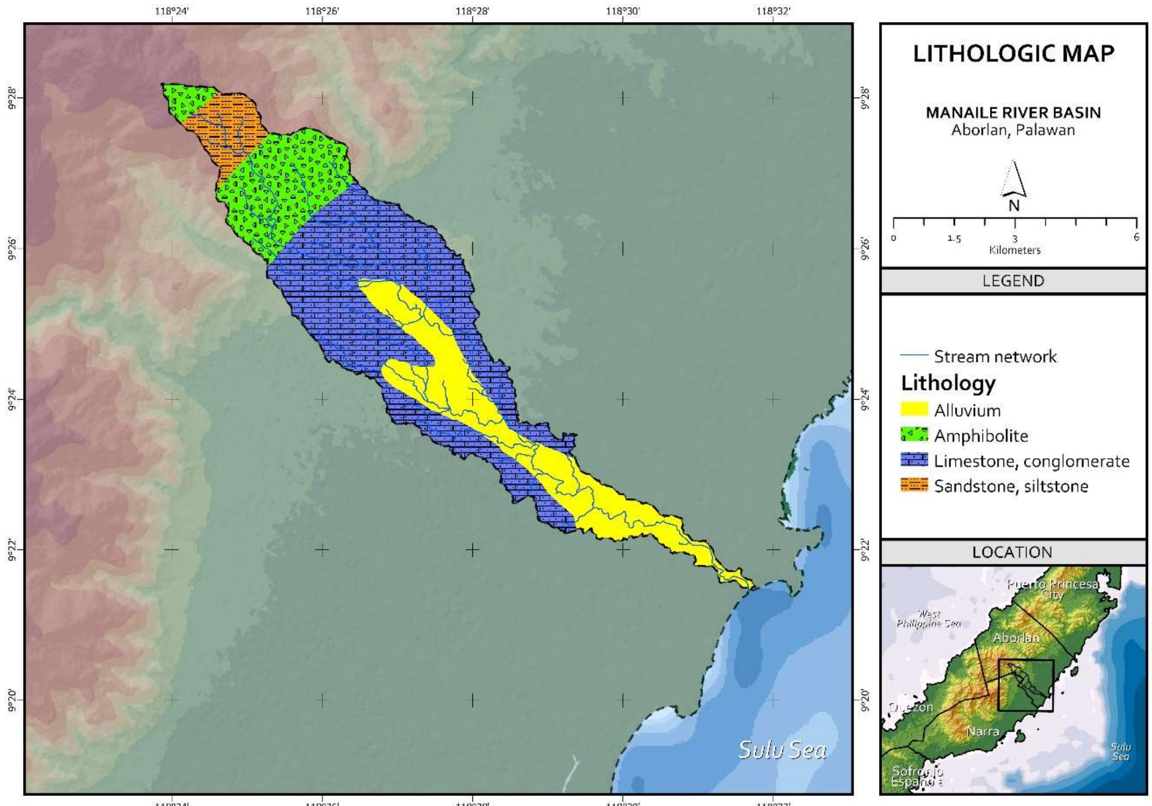

FIGURE 2.6. LITHOLOGIC MAP OF THE MANAILE RIVER BASIN

2.2 Determination of Potential Groundwater Recharge Areas

In general, moderate to high groundwater recharge potential in the Manaile River Basin are found within its catchment. This is in part because of the flat terrain coupled with the permeable limestone lithology found extensively in the catchment. The computed volume of rainwater infiltrating into the ground is 27.8% which will lead to very productive aquifers in the area fed by both rainwater infiltration as well as water from the river itself.

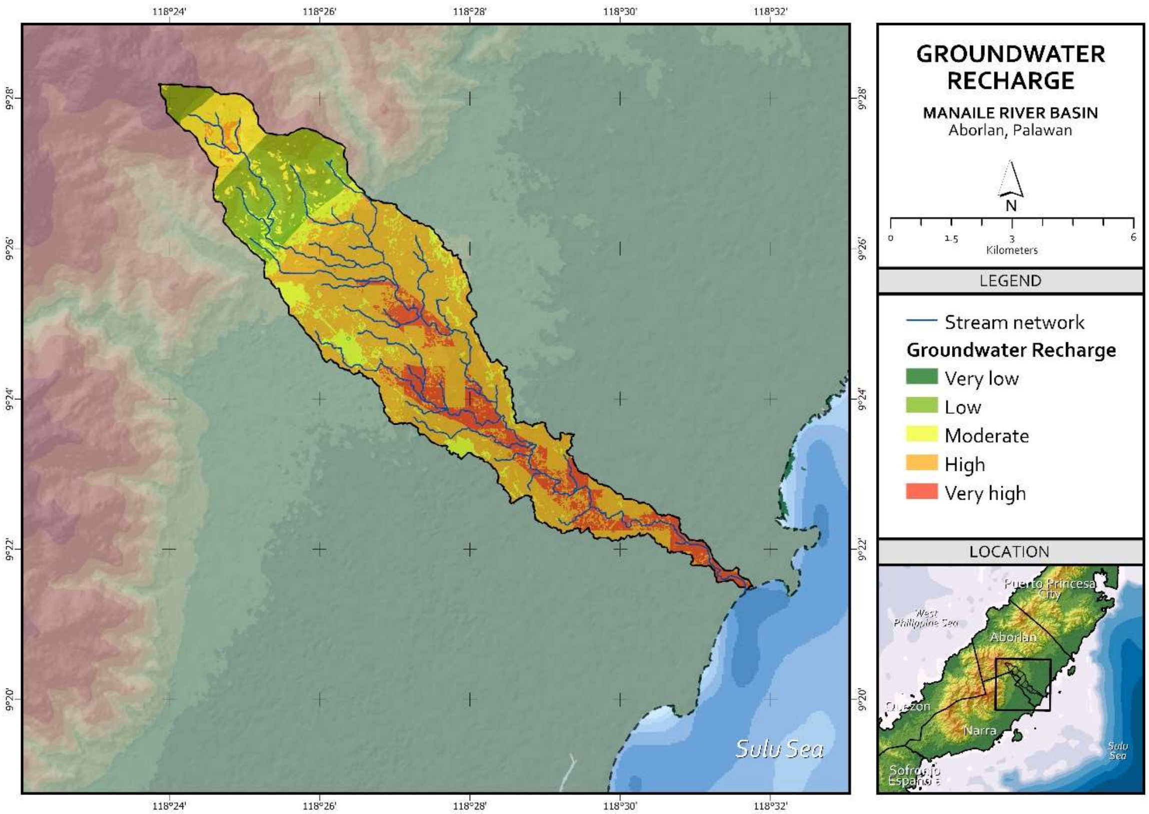

FIGURE 2.7. GROUNDWATER RECHARGE POTENTIAL MAP OF THE MANAILE RIVER BASIN

Between the baseline years of 1976 to 2005, the Manaile River Basin received around 1,369.3 mm of rainfall annually, typical of a Type 3 climate. Based on the 2 scenarios of climate projections: RCP 4.5 (stabilization scenario) and RCP 8.5 (high-emissions/business as usual scenario) for the years 2006-2035 and 2036-2065, the expected volume of recharge is estimated to decrease by up to 13.5% at the end of 2065 (Table 2.1).

During the 1st scenario (RCP 4.5: 2006-2035), groundwater recharge is expected to decrease by up to 4.3% from the baseline years. A further decrease in groundwater recharge of up to 8.6% is estimated to occur during the next 30 years of the stabilization scenario (2036-2065). After 2065, a total of 12.5% decrease in volume of groundwater recharge from the baseline is projected to take place. For the high-emissions scenario (RCP 8.5: 2006-2035), groundwater recharge to the basin is expected to decrease by up to 5.9%, higher than what the stabilization scenario should predict. At the end of the next 30-year period, in 2065, up to 8.0% further decrease in the volume of groundwater recharge is anticipated to occur, translating to a total of up to 13.5% decrease from the baseline period.

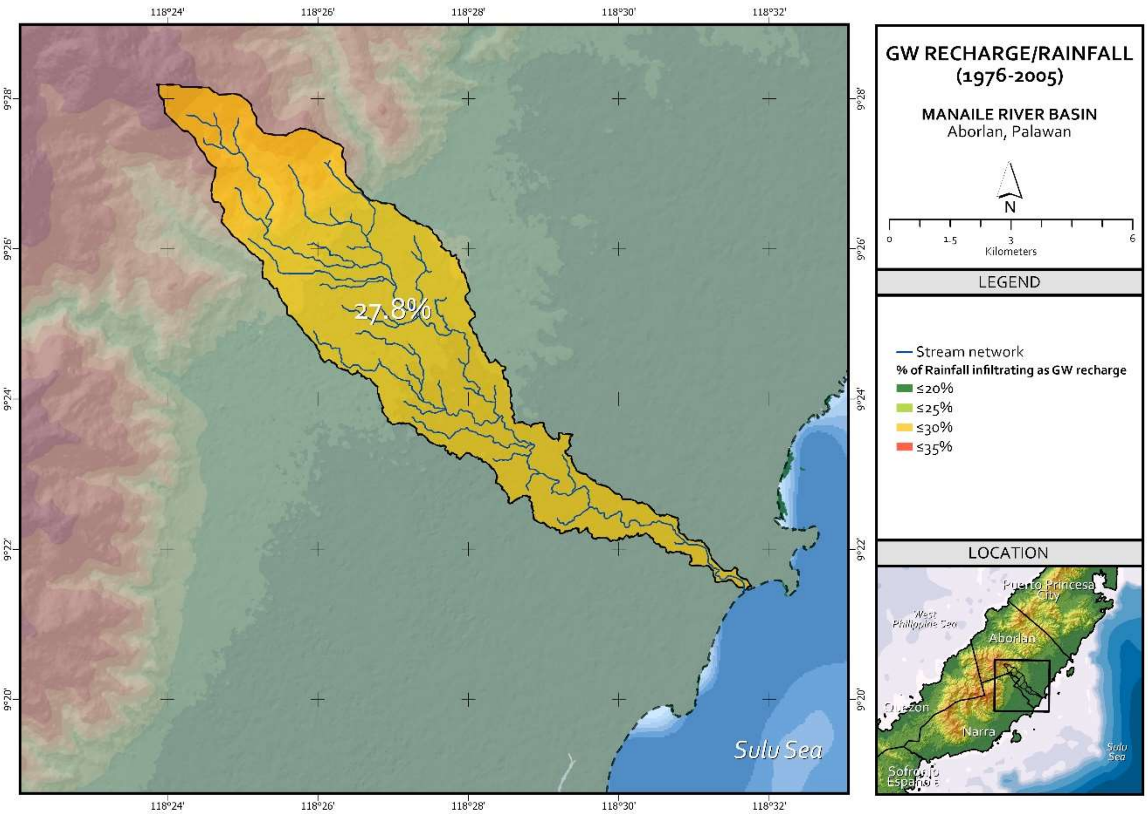

FIGURE 2.8. PROPORTION OF RAINFALL POTENTIALLY INFILTRATING AS GROUNDWATER RECHARGE IN MANAILE RIVER BASIN. THE LABEL (27.8%) INDICATES THE AVERAGE PROPORTION OF RAINFALL INFILTRATING AS GROUNDWATER RECHARGE DURING THE BASELINE YEARS (1976-2005)

TABLE 2.1. PROJECTED VOLUME OF GROUNDWATER RECHARGE OF THE MANAILE RIVER BASIN BASED ON 2 CLIMATE CHANGE PROJECTIONS

	Baseline (1976-2005)	**RCP 4.5 (2006-2035)**	**RCP 4.5 (2036-2065)**	**RCP 8.5 (2006-2035)**	**RCP 8.5 (2036-2065)**
	Volume of recharge reported in cubic meters (m^3)				
Manaile	14,793,793.98	14,156,135.80	12,943,879.15	13,922,449.21	12,802,446.06

SECTION 3: POLICY RECOMMENDATIONS

Based on the mean value of the three flow analysis methods, Manaile River has a calculated 80% dependable flow of 0.22 $m^3 s^{-1}$. Currently, there is a single permittee (0.176 $m^3 s^{-1}$) that utilizes almost the entire dry season flow for irrigation purposes. Similar to small rivers in Palawan with Type 1 climate, Manaile River will be prone to extreme dry conditions during the first quarter of the year as well as during drought conditions due to El Niño events.

In terms of the river's protection of water volume and water quality, the following are our recommendations:

- Augment extraction of water from the river with groundwater by installing shallow groundwater wells for the community's use;
- Monitor users of the river even those that are not registered with the NWRB. This is for managing flow and ensuring that everyone is able to derive their needed volume of water from Manaile River even during drought conditions;
- Provide programs that will lead to bank stabilization and reduction of any pollutants entering the river.

References

Deepa, S., Venkateswaran, S., Ayyandurai, R. et al. Groundwater recharge potential zones mapping in upper Manimuktha Sub basin Vellar river Tamil Nadu India using GIS and remote sensing techniques. Model. Earth Syst. Environ. 2, 137 (2016). https://doi.org/10.1007/s40808-016-0192-9.

Kourgialas, N., Karatzas, G. Groundwater contamination risk assessment in Crete, Greece, using numerical tools within a GIS framework. Hydrological Sciences Journal 60(1), 111-132 (2015). https://doi.org/10.1080/02626667.2014.885653.

Kotchoni, D.O.V., Vouillamoz, JM., Lawson, F.M.A. et al. Relationships between rainfall and groundwater recharge in seasonally humid Benin: a comparative analysis of long-term hydrographs in sedimentary and crystalline aquifers. Hydrogeol J 27, 447–457 (2019). https://doi.org/10.1007/s10040-018-1806-2.

Ministry of Public Works and Highways. Design Guidelines Criteria and Standards, Vol.1 (1987). In: Department of Public Works and Highways (DPWH) and Japan International Cooperation Agency (JICA). Manual on Flood Control Planning, March 2003.

Neri, M., Le Cozannet, G., Thierry, P., Bignami, C., and Ruch, J.: A method for multi-hazard mapping in poorly known volcanic areas: an example from Kanlaon (Philippines), Nat. Hazards Earth Syst. Sci., 13, 1929–1943, https://doi.org/10.5194/nhess-13-1929-2013, 2013.

Senanayake, I.P., Dissanayake, D.M.D.O.K., Mayadunna, B.B., Weerasekera, W.L. An approach to delineate groundwater recharge potential sites in Ambalantota, Sri Lanka using GIS techniques. Geoscience Frontiers 7(1), 115-124 (2016). https://doi.org/10.1016/j.gsf.2015.03.002.

Shaban, A., Khawlie, M. & Abdallah, C. Use of remote sensing and GIS to determine recharge potential zones: the case of Occidental Lebanon. Hydrogeol J 14, 433–443 (2006). https://doi.org/10.1007/s10040-005-0437-6.

Yeh, HF., Lee, CH., Hsu, KC. et al. GIS for the assessment of the groundwater recharge potential zone. Environ Geol 58, 185–195 (2009). https://doi.org/10.1007/s00254-008-1504-9.